Brain Disorders 13 (2024) 100112

Contents lists available at ScienceDirect

Brain Disorders

journal homepage: www.sciencedirect.com/journal/brain-disorders

MRI tractographic validation of drug-enhanced hepatic clearance of amyloid-beta and the therapeutic potential for Alzheimer's Disease: A pilot study

Anindita Bhattacharjee [a], Prasun K. Roy [b,c,*]

[a] School of Bio-Medical Engineering, Indian Institute of Technology (B.H.U.), Varanasi 221005, India
[b] Department of Life Sciences, Shiv Nadar University (Institution of Eminence), Delhi NCR, 201314, India
[c] SNU-Dassault Systemes Centre of Excellence, Shiv Nadar University (Institution of Eminence), Delhi NCR, 201314, India

ARTICLE INFO

Keywords:
Diffusion tensor imaging
Braak's stages
Metformin
Cilostazol
Rifampicin
Liver
Bile

ABSTRACT

Alzheimer's disease (AD) may require alternative therapeutic perspectives as current interventions may sometimes be sub-optimal. Amyloid-beta 42 ($A\beta_{42}$) is mainly eliminated by hepatic clearance which diminishes in AD, hence hepatomodulatory drugs enhancing this clearance may have potentiality for therapeutic implication. Here, we clinically substantiate our systems-biology investigation on repurposed hepatomodulating drugs (metformin, cilostazol and rifampicin) which enhance brain insoluble $A\beta_{42}$ clearance through liver-bile-faeces route. Through MRI-tractographic analysis, we now formulate a three-segmental basis of brain $A\beta_{42}$ spread: fronto-thalamic region (segment-1), temporo-occipital region (segment-2), and dorso-cingulate region (segment-3). This segmental pattern is corroborated histopathologically by Braak's stages A, B and C. We further observed that the aforesaid three pharmaceuticals respectively acted on those three segmental regions differentially. We analysed MRI and DTI images of 15 healthy controls (CDR: 0; MMSE: 24–20), and 15 AD patients (CDR: 0.5–1.0; MMSE: 20–26). We found that, tractographically, there is a significant reduction in neuronal integrity in the three aforesaid regions in untreated AD compared to controls. Nevertheless, the three drugs increased neural activation of AD patients in the three corresponding areas. These three drugs act by regulating respectively the genes *ABCB11, ABCA1* and *MDR1*. These genes were correspondingly downregulated in the above-mentioned anatomical segments 1, 2 and 3 of Alzheimer's disease. Thus personalized patient-specific hepatomodulative drugs for AD intervention may be explored, as corroborated by the neuroanatomical involvement in AD.

1. Introduction

Alzheimer's disease (AD) beckons a different therapeutic approach because newer treatments for AD using neurological medications may not always produce the desired results. It is now known that AD is actuated by amyloid-beta ($A\beta_{42}$) accumulation rather than $A\beta_{42}$ formation, and a main pathogenesis is due to reduction of $A\beta_{42}$ elimination, which occurs primarily through the liver into bile and faeces [1–3]. Furthermore, clinical trial investigation shows that liver damage decreases $A\beta_{42}$ clearance from blood [4], and it is also known that hepatic dysfunction can induces sign of AD (Kim et al., 2026). In other words, it can be taken that hepatomodulatory drugs which can enhance this hepatic clearance of $A\beta_{42}$ may be a physiological therapeutic approach to AD. Animal studies show that hepatic $A\beta_{42}$ clearance reduces in AD and those drugs can reduce brain $A\beta_{42}$ and reverse behavioural-cognitive deficits of AD [5]. Hence, we may infer that these drugs might also have potentiality to alleviate human AD. We have earlier developed robust systems biological approach to this aspect, showing that hepatic clearance of brain $A\beta_{42}$ clearance can be enhanced via three pathways: (a) Pregnane-X-receptor, (b) Bile salt export- pump receptor, and (c) Phosphodiesterase inhibition, and these pathways can be activated respectively by three candidate molecules: (i) Rifampicin, (ii) Metformin, and (iii) Cilostazol [6] (Fig. 1).

Furthermore, we have earlier developed a histologically-validated MRI diffusion tensor imaging (DTI) approach showing that axonal white matter tracts may function as migration scaffold in human brain [7]. Numerous laboratories, including ours, have shown that such axonal scaffolds furnishes the substratum for transport of migratory

* Corresponding author at: R-206, Department of Life Sciences, Shiv Nadar University (Institution of Eminence), NH-91, Delhi NCR, 201314, India.
E-mail address: prasun.roy@snu.edu.in (P.K. Roy).

https://doi.org/10.1016/j.dscb.2023.100112

Available online 1 January 2024

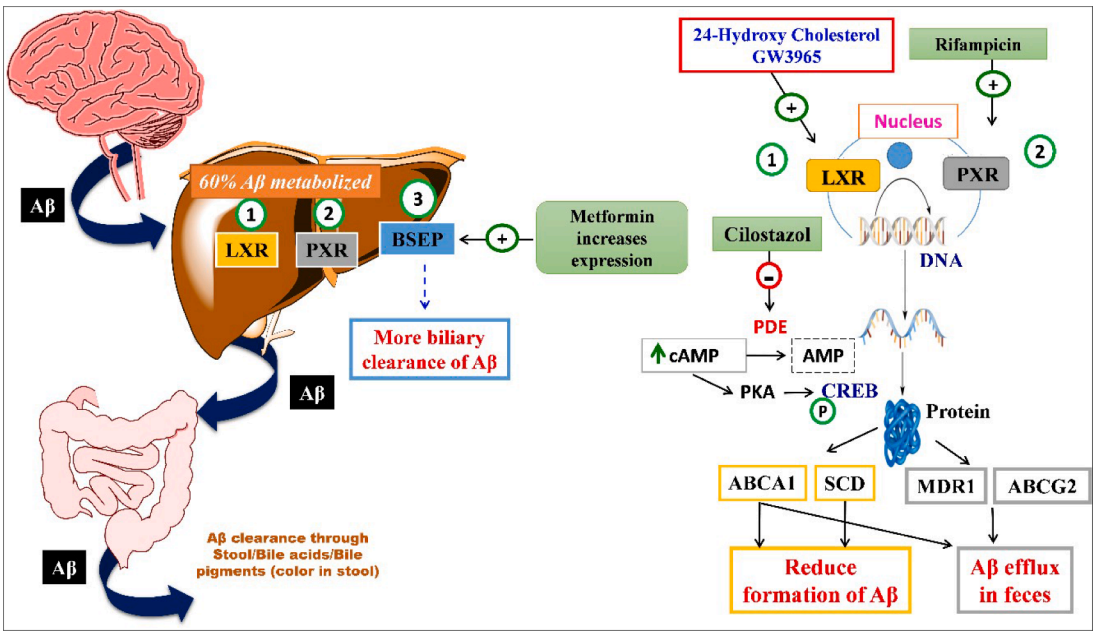

Fig. 1. Schema of the three pathways of the hepato-biliary-faecal elimination route of $A\beta_{42}$ of brain, each pathway can be enhanced by a corresponding pharmacological agent.

entities, whether $A\beta_{42}$, prion protein, stem cells or virus [8–10]. Hence, we can take that this MRI tract network can also be a scaffold for $A\beta_{42}$ spread in brain, moreover so as rodent models show that $A\beta_{42}$ and prion spread occurs along axons¸ which is accompanied by neurotoxic effects as endosomal leakage, tubulin beading and neurite damage [11].

2. Methods and analysis

2.1. Analysis of clinical trial findings and neuroimaging scans

We analysed the neuroimaging scans and clinical findings of three clinical trials of AD under the action of three hepatomodulatory amyloid-beta clearance agents (metformin, cilostazol and rifampicin) [12–14]. According to the images, we observe that these three drugs

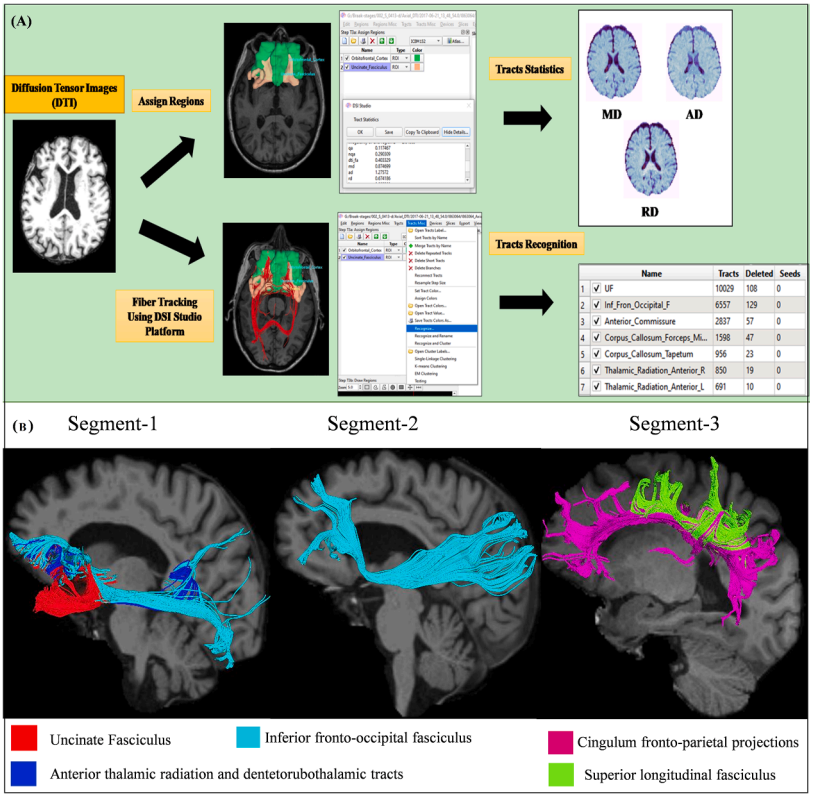

Fig. 2. (a) Imaging analysis procedure for diffusion tensor imaging, and (b) Tractography and identification of the fibres in the three segments of the brain.

stimulate different brain regions in AD patients, with the dominant activation respectively being in three zones: (i) Segment-1: Metformin activates the orbitofrontal and uncinate region [13]; (ii) Segment-2: Cilostazol activated the parietal and inferofrontal region [14]; (ii) Segment-3: Rifampicin activated the posterior cingulate and parietal association area [12].

2.2. MRI data acquisition

The Alzheimer's Disease Neuroimaging Initiative (ADNI) database was used to obtain structural MRI and DTI data for cognitively normal (CN) and Mild Alzheimer's Disease dementia (AD) subjects used in the present study [15]. The ADNI program was launched in 2004 as an multicentric clinical cooperation as a private-public partnership. The principal objective of this initiative was to develop clinical, imaging, genetic, and biochemical biomarkers for the early detection and monitoring of AD. We have analysed diffusion MRI scans from the ADNI database (http://adni.loni.usc.edu) of 30 subjects (15 healthy controls and 15 AD CE patients) [it may be mentioned that we had calculated the sample size of this study and we found that the minimum size required is $n_1 = n_2 = 13$, see Supplementary information; hence it can be taken that our sample size is satisfactory]. The subjects were classified using mini-mental state evaluation (MMSE) and global clinical dementia rating (CDR) scores [16]. The control participants (healthy subjects) had Mini-Mental Status Examination (MMSE) scores of 24–30 and a Clinical Dementia Rating (CDR) score of 0. Similarly, for Alzheimer's subjects, MMSE score was between 20-26 and CDR of 0.5–1.0. The Institutional Review Board approved this study of all the participants. Informed written consent was obtained from all subjects. We included subjects whose baseline DWI and T1- weighted MRI scans were accessible. For all participants, whole-brain MRI scanning was performed using a range of various 3T Medical Systems made by GE, Siemens, and Philips. For each DTI scan, two sets of ten images were obtained: ten diffusion-weighted images ($b = 1000 s/mm^2$) and ten T1-weighted images without diffusion stimulation (b0 images). Two distinct acquisition protocols are outlined for DWI scans: According to the "IDA_MR_Metadata_Listing.csv" file on the ADNI website, 1) Axial DTI and 2) Enhanced Axial DTI. On ADNI's main website, you can find more information about the data acquisition procedures for its MRI scanners.

2.3. Tractography analysis

The diffusion MRI data were pre-processed with DSI-Studio software (Fig. 1(a)). This platform is used for deterministic fibre tracking, reconstruction, and three-dimensional visualisation (http://dsi-studio.labsolver.org). The restricted diffusion was measured using restricted diffusion imaging procedure. The diffusion data were reconstructed using generalised q- sampling imaging (GQI) with a diffusion sampling length ratio of 1.25. The anisotropy threshold was 0.02. The angular threshold was 60°. The step size was 0.1 mm. Tracks with length shorter than 5 or longer than 300 mm were discarded [17].

2.3.1. Mapping of tracts

Segment-1. Regarding the mapping of the aforesaid anatomical segment-1, one ROI was placed in orbitofrontal cortex, and another ROI in uncinate region. The tracts were constructed using the deterministic tractography tools [Tracts] [Tracts to ROI]. Then the tract misc tool was used for recognizing and clustering the tracts. This tool uses the a tractographic atlas for processing [18]. Subsequently, identification and nomenclature of the tracts were undertaken using the menu [Tracts] [Miscellaneous][Recognize Track]. Also, the tract metrics were obtained using the function [Tracking Parameters][Differential Tracking][Metrics] option of DSI studio. The left panel of Fig. 2(b)in the text shows the tracts obtained from an AD patient, and these tracts were identified as uncinate fasciculus, anterior thalamic radiation, and rubrothalamocerebral tract.

A similar procedure was performed for the anatomical Segments 2 and 3, and likewise the tracts were constructed and identified as follows:

Segment-2. ROI is placed at parietal lobe and another ROI at inferior frontal region. Thereby, in an Alzheimer's subject, we obtained and identified the inferior occipital fasciculus whose fibres pass to temporal region (Fig. 2b, middle panel).

Segment-3. An ROI was placed respectively at posterior cingulate cortex and one at parietal association cortex. Thereby, we arrived at the cingulum fronto-parietal projection tract and superior longitudinal fasciculus (Fig. 2(b), right panel).

2.4. Genetic association analysis

Microarray data for Alzheimer's Disease genes formulated in our approach (ABCG2, ABCB11, ABCA1, MDR1, SCD and ASBT) in post-mortem human brain tissue of the normal adults were downloaded from the human brain transcriptome database of the Allen Brain Atlas (https://human.brain-map.org/). Microarray survey, data normalization and platform selection along with the ontology and nomenclature of anatomical structures of brain were mentioned in the Allen brain atlas platform (Documentation - Allen Human Brain Atlas (brain-map.org). The brain regions where upregulation and downregulation of proposed genes occur were identified based on expression levels. Detailed methodology is in Supplementary material-S3.

3. Results

3.1. Clinical trial analysis

Our analysis of the clinical findings and neuroimaging scans of item 2.1 revealed the three different segments of brain were activated by the corresponding three drugs (metformin, cilostazol and rifampicin). Supplementary Table S4 represents information of our systems biology analysis and the clinical trials. Analysing those above-mentioned scans, we find that these three drugs activate different neural regions in AD patients with the dominant activation being respectively in following three zones. (a) *Segment-1*: Activation of areas as orbitofrontal and uncinate region by Metformin, thereby improving learning/memory ($p = 0.044$) [13]. In their study Koeing et al. reported increasing orbitofrontal cerebral blood flow after metformin treatment, as estimated by MRI-ASL perfusion study. Their cognitive testing (ADAS-Cog and CANTAB-PAL tests) also revealed improvement in learning and memory as well as in executive functioning in AD subjects after treatment with metformin; (b) *Segment-2:* The FDG-PET study conducted by Lee et al. reported that activation of areas as parietal region and inferofrontal region by Cilostazol, with notable glucose metabolism increase ($p = 0.005$) [14]; moreover, psychological testing by ADAS-Cog scoring showed definitive improvement; (c) *Segment-3:* Iizuka et al. revealed in their FDG-PET analysis that activation of areas as posterior cingulate and parietal association area by Rifampicin, whose metabolic change between 12-and 6-month therapy was markedly enhanced ($p = 0.009$); here cognitive assessment by MMSE showed appreciable affirmative effect [12].

3.2. Deterministic tractography

We then separately constructed for each segment (1, 2 and 3) the fibre tracts using deterministic tractography. Thereafter, we performed the identification and nomenclature of the nerve tracts corresponding to those three segments as follows (Supplement- S1) (Fig. 2(a)and Fig. 2 (b)). (A) *Segment 1:* Uncinate fasciculus, anterior thalamocortical radiation, and thalamocerebral tract (as dentatorubothalamic) tract; (B) *Segment 2:* Inferior fronto-occipital fasciculus (IFOF) leading to the occipito-patietal region. It is known that IFOP tract also connects to

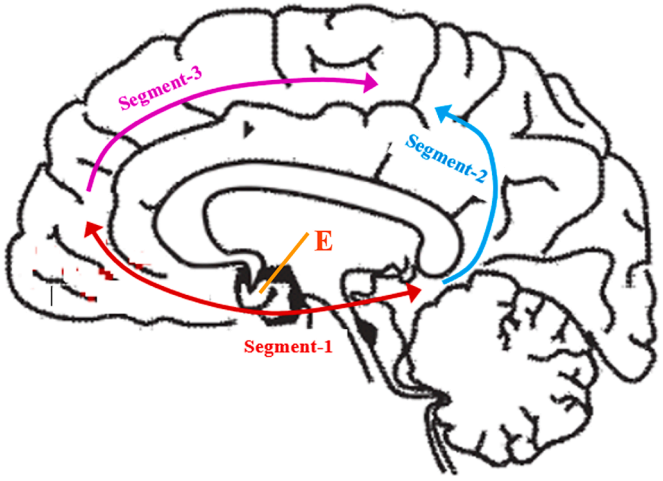

Fig. 3. Geometric motif of the white matter tract profile providing the neural fibre scaffold for Aβ42 migration circumferentially across the cerebrum, with the three schematic segments shown. The Aβ42 deposition starts at entorhinal-uncinate region E and migrates bidirectionally as segment-1 and then circles across the cerebrum, by segments 2 and 3.

parietal lobe and temporal lobe (hippocampus), and is part of fronto-parietal network [19]; (C) *Segment-3:* Cingulum's fronto-parietal projections and superior longitudinal fasciculus dorsally.

Anatomically, it is known that the uncinate fasciculus adjoins the entorhinal cortex (EC). Indeed, entorhinal cortex is a most vulnerable region for AD, as it is juxtaposition between allocortex and neocortex, and is the initial area where $A\beta_{42}$ is first formed in AD, due to mitophagy-induced death of entorhinal neurons [20]. Accordingly, we can construe that $A\beta_{42}$ spread in brain will initialize in EC and then traverse by the white-matter fibre of uncinate and anterior thalamic/rubrothalamocerebral tracts (Segment-1). Levitis et al. reported that the default mode network (Segment-2,3) is the focal zone of amyloid beta spread in sporadic AD and most autosomal-dominant AD patients express amyloid-beta spreading patterns similar to those of sporadic AD. [21]. We now explore the full gamut of $A\beta_{42}$ spread via the aforesaid white matter tracts (Fig. 2(b)) and note the three segments may enable $A\beta_{42}$ spreading via a circumcerebral pattern:

(i) *Segment-1*: Anterior portion of the tractography from uncinate faciculus, rubrothalamocerebral tract and anterior thalamic radiation, leads forward to neocortex region, as orbitofrontal/inferior frontal cortex, and frontal area of anterior cingular region;
(ii) *Segment-2*: Posterior portion of the tractography from inferior fronto-occipital fasciculus leads towards the allocortex region, as limbic system, e.g. posterior cingular area, and to temporo-occipital-parietal region;
(iii) *Segment-3*: Tractographic fibre of the superior longitudinal fasciculus and the cingulum's fronto-parietal projection are found to traverse supracallosally and interlink the frontal with the occipito-patietal region of the brain. Indeed, the anterior and posterior cingular fibres (segment-1 and 2 respectively) meet supracallosally around the vertex sensorimotor region. In other words, the amyloid spreads via tracts of the three segments forming a circumcerebral route around the brain as delineated in Fig. 3.

3.3. Histopathological validation using braak staging

We now show how the schematic prediction of Fig. 3 and its three tractographic segments are corroborated by Braak et al.'s corresponding three histopathologically-confimed time-wise stages A, B and C of

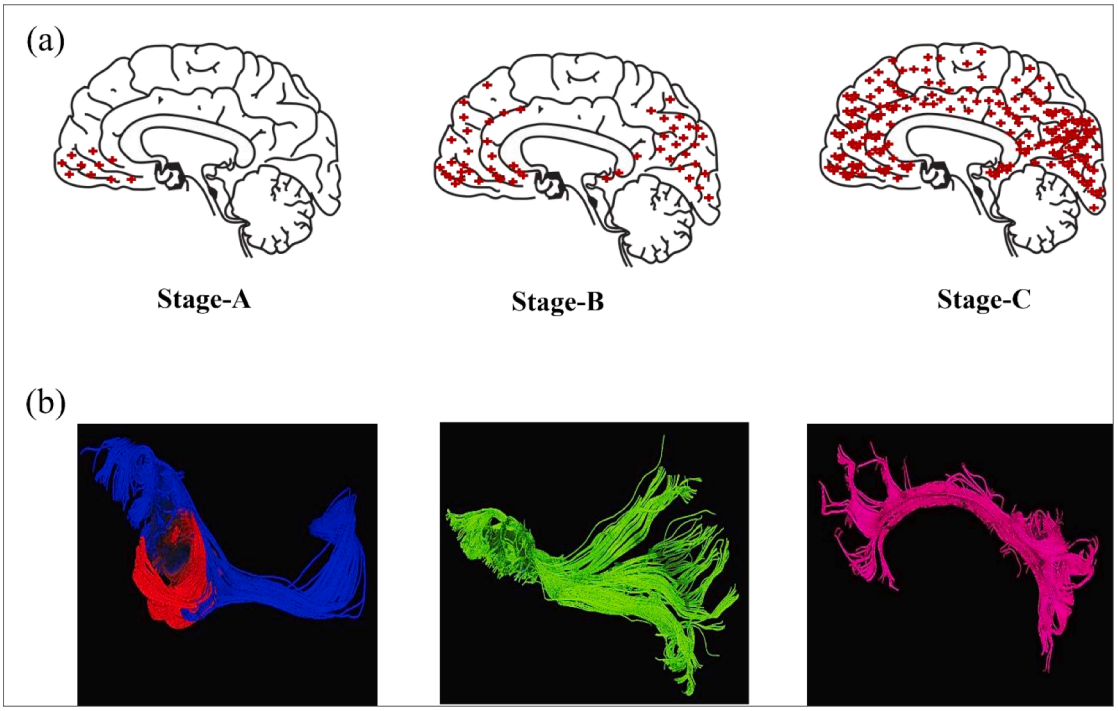

Fig. 4. (a) Aβ42 distribution in the stages as Alzheimer's disease progresses over time, as observed by microscopic histopathological examination of Aβ42 plaques denoted by red markings. Braak Stage-A begins with initial Aβ42 deposits in the isocortex, as the basal zones in frontal and temporal regions. Stage-B shows Aβ42 gradual spread into ventral two-thirds portion of the frontal, temporal, occipital and parietal regions, including the isocortical association areas, except the superior cerebral portion as the sensory and motor regions in the dorsal vertex. Stage-C is late-stage situation where Aβ42 spreads throughout the cerebral isocortex, including primary sensory and motor region in the cerebral dorsal vertex, (b) The corresponding nerve fasciculus that may act as scaffolds for the amyloid migration, the fascicles being obtained by DTI tracking (the three panels of fasciculus here correspond respectively to the amyloid migration in the three Braak stages).

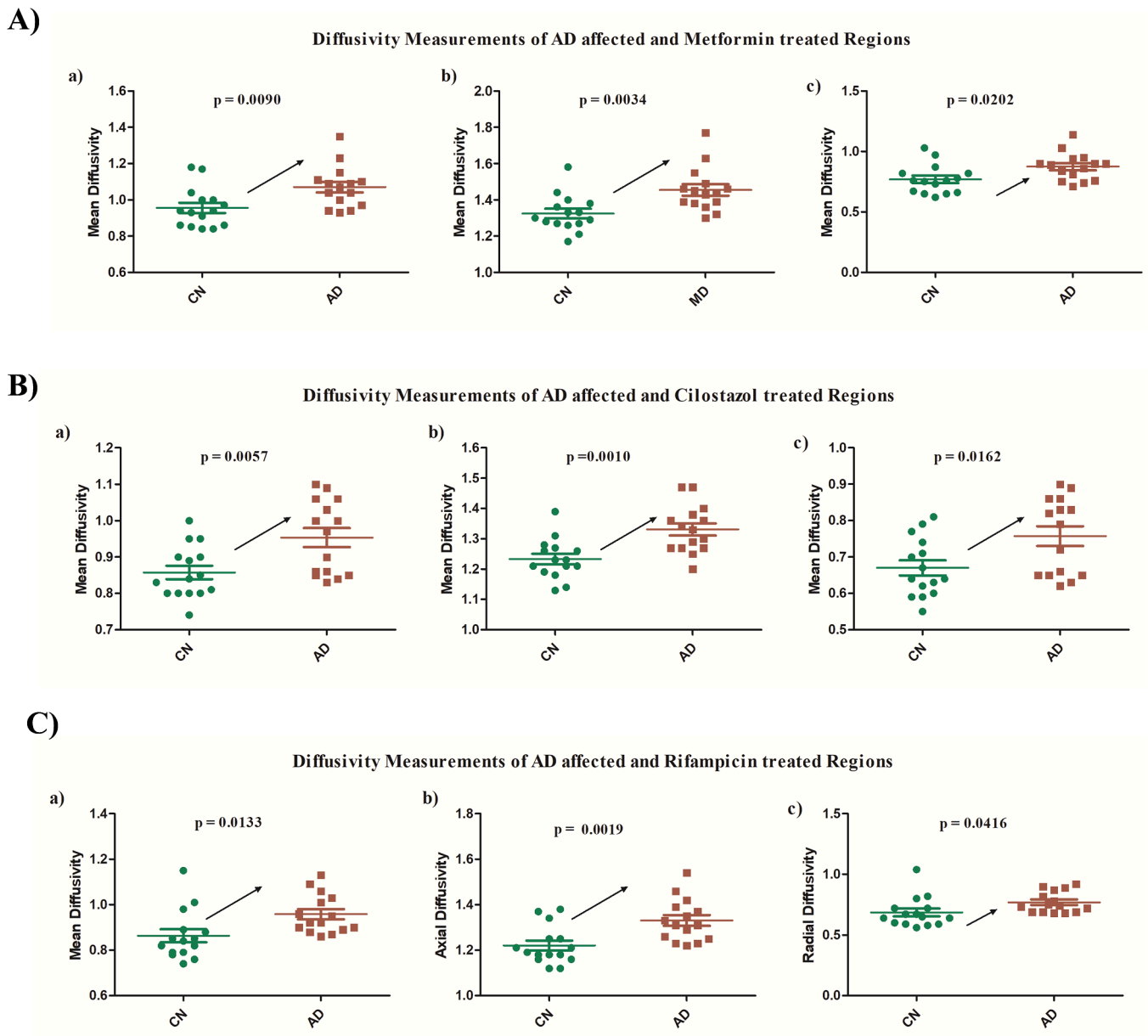

Fig. 5. Neural tract impairment in AD patients at (A) Segment-1, (B) Segment-2, and (C) Segment-3. The panels show that diffusivity indices increases in AD subjects over controls: (a) Mean Diffusivity, (b) Axial Diffusivity, and (c) Radial Diffusivity. The rise of diffusivity is of high statistical significance ($p \leq 0.005$), together with large effect size.

cerebral $A\beta_{42}$ spread in AD. The Braak procedure involves microscopic examination of microtome-sectioned AD brains embedded in polythene glycol and then stained for amyloid beta using the standard Bodian silver staining and lipofuscin. As per their formulation [22]: *Stage-A* mainly involves ventral basal region of temporal and frontal lobes; *Stage-B* chiefly incorporates ventral two-thirds of frontal, occipital and parietal (association) regions; *Stage-C* involves remaining regions, primary sensory and motor region in cerebral vertex (Fig. 4a).

One notes that the Braak stages A, B and C well concurs respectively with our tractographic segments 1, 2 and 3 (Fig. 4b). We show in Fig. 4b the corresponding nerve fasciculus obtained by DTI tracking as per methodology of Fig. 2b. Indeed, Segment-1 tracts includes the thalamus, and this thalamic involvement in the incipient AD process is corroborated by thalamic morphometry measurements [22]. Furthermore, the circumcerebral aspect of tractographic pathway is also closely substantiated by the circumcerebral Papez circuit- based formulation of AD pathogenesis, supported by electrophysiological and PET imaging findings [23]. To recollect, the Papez circuit is the C-shaped affective/emotive/memory pathway, traversing entorhinal cortex, prefrontal region, cingulum, and thalamus. Of especial note, is that the dysfunction of dorsal pathway (Segment-3) is corroborated by fMRI and molecular imaging in AD/MCI showing hypoactivation of cingulate region [24,25]. Indeed, the segments 1, 2 and 3 correlate respectively with the functional nodes of default-mode network (frontal, parietal and cingulate hubs), and it may be mentioned that these hubs become impaired in AD [26].

3.4. *Alteration of fibre tracts in Alzheimer's Disease*

We then identified the fibre alteration in the aforementioned tractographic segments 1–3 in AD subjects. We estimated the tract diffusivities (axial, radial, mean diffusivities) in AD vis-a-vis control subjects. For this comparison, we used diffusion MRI scans of 30 subjects (age-matched/sex-matched 15 healthy and 15 AD subjects) from AD

neuroimaging system (Supplement-S2). We also performed effect size assessment and power analysis of tract parameters of these subjects and found that 13 subjects of each group would be sufficient for statistical analysis (Supplement-S2). Indeed, all our AD vis-à-vis control differences were highly significant ($p \approx 0.005$) with large effect-sizes, as delineated below. Using DTI analysis, we found that the tract systems of Segments 1–3 show considerable neural damage in AD with respect to controls, as follows.

Segment-1: Uncinate and orbitofrontal tracts were impaired in AD with significantly higher diffusivity parameters (axial, radial and mean-diffusivities) ($p < 0.004$, Fig. 5A), thus indicating fibre damage and axonal transport impairment. Our observation is correlated by histopathological studies showing that Wallerian-type neuronal degeneration occurs in AD [27]. Nevertheless, the anatomical region of segment-1 improved significantly by metformin treatment in AD ($p = 0.044$) (Section 3.1).

Segment-2: Likewise, in AD patients we observed increased diffusivity-based neural tract impairment in the parietal and inferior frontal regions ($p < 0.005$; Supplementary Table S2). To underscore, the functioning of these regions is enhanced in AD subjects under cilastozol therapy ($p = 0.005$) (Section 3.1) (Fig 5B).

Segment-3: Similarly, we found that fibre dysfunctionality is revealed by higher diffusivities in the posterior cingulate and parietal association regions ($p < 0.005$, Supplementary Table S3). Moreover, the functionality of these regions improved by rifampicin treatment in AD subjects ($p = 0.009$) (Section3.1) (Fig. 5C).

3.5. Gene expression analysis

Thereafter, we analysed the target genes of the three drugs. As elaborated in the Introduction, we have earlier found that these drugs hepatically excrete $A\beta_{42}$ by activating the following respective genes: (i) Metformin: ABCB11; (ii) Cilostazol: ABCA1 and SCD; and (iii) Rifampicin: MDR1 and ABCG2 [6]. To investigate the collateral expression of these genes in brain, we analysed Allen Brain-Atlas (Human system). We found that in the senescent brain (ageing-induced neurodegeneration), these genes are downregulated differentially in separate brain regions (Supplement-S3). Therein, the gene ABCB11 is downregulated by 64% in Segment-1 (and not in segments-2,3) (Supplement-S3). To recall, ABCB11 is metformin's target gene whose expression enables hepatic $A\beta_{42}$ clearance from blood to bile via hepatocytes in livers. In AD, this gene may be downregulated [26], and metformin may induce it to become upregulated (Fig. 1), this upregulation ensues with actuation of the BSEP system, the bile salt export pump process [6,28]. The former investigation [28] deals with a microarray study from ABCB11 knockout mice, and validation was done on human liver cells, along with real-time PCR analysis and Western Blot against anti-human ABCB11 antibody. It may be mentioned that this same gene ABCB11 is downregulated only in segment-1, the part of the brain that is affected in AD but can be activated with metformin treatment. From an integrated perspective, the ABCB11 gene expresses in both liver and cerebral segment-1, and is dysfunctional and downregulated in AD, and beneficial upregulation can occur by metformin. Indeed, functioning of the same gene in different tissues may occur by alternative splicing and epigenetic processes [29]. ABC families, including ABCB11, are also subject to alternative splicing, which may have ramifications for their differential expression in various types of tissues [30]. Indeed, both liver and brain are two organs where these differential splicing levels are much higher than other tissues [31]. To give another example, the classical fibronectin FN1 gene can also differentially expressed in hepatocytes and neurons using alternative splicing [32].

We thereafter considered genes ABCA1 and SCD (cilostazol). Analysing the Allen Brain-Atlas (Human system), we found that these genes are downregulated in segment-2 (and not in segments-1,3), where segment-2 is cerebral region activated by cilostazol (Supplement-S3).

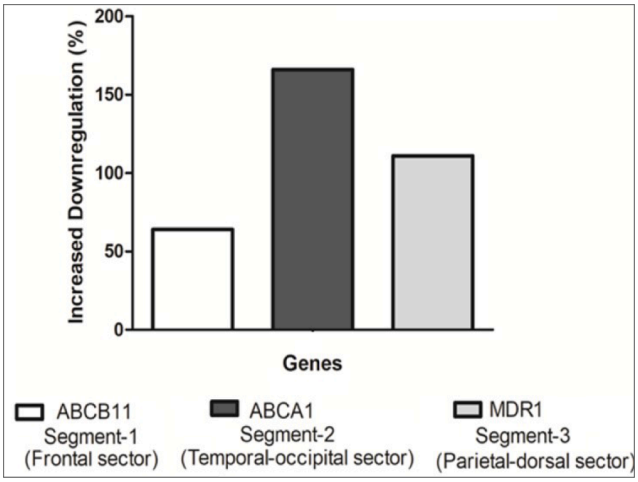

Fig. 6. Intensity of downregulation of the genes ABCB11, ABCA1 and MDR1 respectively in segment 1 (frontal sector), segment 2 (temporal-occipital sector) and segment 3 (parietal-dorsal sector).

Similarly, we observed that genes MDR1 and ABCG2 (rifampicin) are downregulated only in segment- 3, the region activated by rifampicin (Supplement-S3). To exemplify, we plot the downregulation level of genes ABCA1 and MDR1 in senescent human brain (Fig. 6). These genes are also downregulated in AD [33,34]. Supplementary Table S5 summarizes our findings.

To paraphrase, we can mention that our genetic analysis above as well as our earlier observations (see Introduction) delineate that the major route of elimination of amyloid-beta from the brain is as follows. The amyloid-beta proceeds from the brain to the blood and thence to the liver, thereafter to the bile, and then to the intestine, and finally exiting through the faeces. Indeed, investigations show that AD is actuated by amyloid-beta ($A\beta_{42}$) accumulation, instead of $A\beta_{42}$ production, and a main factor is the decrease of $A\beta_{42}$ elimination, and the $A\beta_{42}$ clearance is mainly a liver-based exit into the bile and faeces [1–3]. Moreover, as mentioned earlier, clinical observation studies indicate that liver damage reduces clearance of $A\beta_{42}$ from the blood [4]. Furthermore, it is well-known clinically that hepatic insufficiency can produce symptoms and signs of AD (Kim et al., 2026). In other words, one can formulate that hepatomodulatory pharmaceutical agents can enhance hepatic amyloid-beta elimination and this route may be pursued as an AD treatment intervention. Actually, preclinical redent investigations [5] confirm that liver-based elimination of $A\beta_{42}$ becomes appreciably less in AD, and those aforesaid pharmaceuticals may diminish the cerebral amyloid-beta, and thereby ameliorate the neurocognitive dysfunction of AD.

4. Discussion

Our findings thus imply an innovative pharmaco-anatomical approach to AD management using a neuroanatomical tract- network perspective. The $A\beta_{42}$ is majorly cleared by faecal route: brain → cerebral blood → liver → bile → faeces. Here, the first and third arrows denote cellular-efflux interfaces (neurovascular pericytes, and hepatocytes respectively). These various alternative $A\beta_{42}$-efflux pathways and gene-sets are expressed at both interfaces, respectively in brain and liver [35], thereby enabling seamless integrated Aβ42-excretion route. Different brain regions may use different pathways which can be enhanced by different drugs (Fig. 7). It is known that AD can be of four forms depending on the location of the anatomical involvement, namely frontal, temporal, parietal, and diffuse-atrophy forms [36]. Analysing several clinical trials [12–14], we have, in Section 3.1, elucidated that the drugs metformin, cilostazol and rifampicin respectively activate segments 1, 2 and 3. Further, the tractography of Section 3.2 delineates

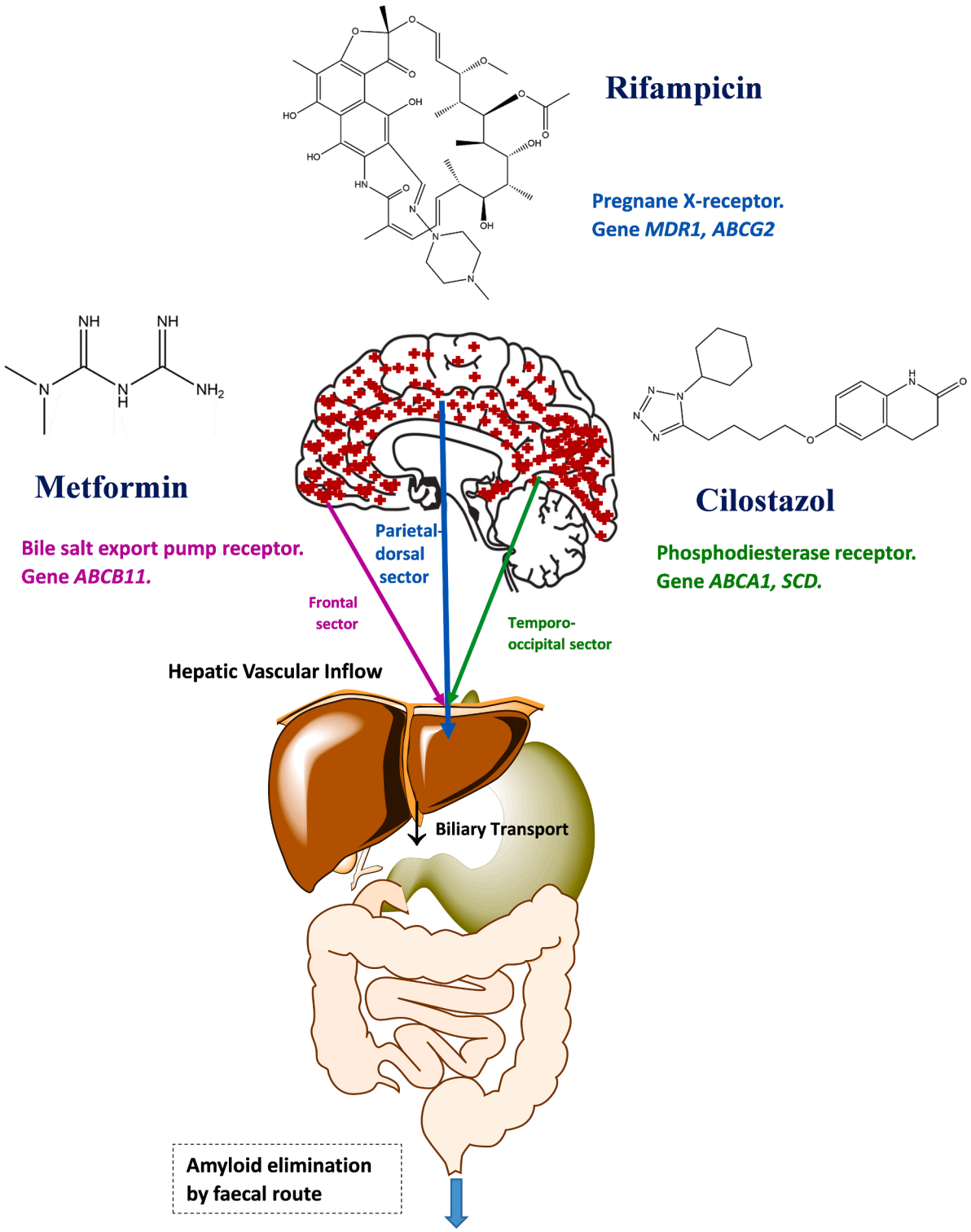

Fig. 7. Physiological routes, receptors and pharmacomodulation of hepatic clearance of Aβ42 from the corresponding brain regions.

that segment 1 is neuroanatomically related with the frontal aspect of the cerebrum (e.g. anterior thalamocortical, uncinate and thalamocerebral tracts), segment 2 is neuroanatomically associated with the temporal aspect of the cerebrum (e.g. hippocampus, and occipitofrontal fibres that pass to the temporal lobe), and segment 3 relates to the parietal region (e.g. parietal projection of cingulate and superior longitudinal fasciculus that links to the parietal portion). In other words, taken together Sections 3.1 and 3.2 indicates that frontal form of AD would affect segment 1, and thus may be amenable to metformin's therapeutic effect. Likewise, the temporal form of AD would involve segment 2, and hence may be suitable for the clinical action of cilostazol. Similarly, the parietal form of AD would affect segment 1, and thus may be feasible for rifampicin's efficacy. On the other hand, the fourth type of AD, the diffuse-atrophy form, is generalized across the various regions of the cerebri (including the temporal, frontal and parietal regions) and so may be suitable for the three drugs combined synergistically (Table 1).

It may be noted that we have basically used two analysis set-ups: (i) subjects from the AD neuroimaging platform, (ii) subjects from the

Table 1
Neuroanatomical forms of AD and corresponding possible personalized pharmacological enhancement of amyloid elimination.

Alzheimer's disease form	Brain regions involved	Anatomical segments associated	Feasibility of hepatomodulative drug
Frontal form	Lateral frontal region	Segment-1	Metformin
Temporal form	Middle and inferiortemporal region	Segment-2	Cilostazol
Parietal form	Lateral parietal, precuneus and cingulate region	Segment-3	Rifampicin
Diffuse atrophy form	Nearly all regions	All three segments	Combination: Metformin, Cilostazol, and Rifampicin

therapeutic investigation using the hepatomodulative drugs. From the first set-up group, we obtained the DTI findings of regions which we related with the regions of the second set-up. It may be underscored that such cross-group generalizability has been well substantiated by other investigators, indeed it is well-known that AD research observations of one study can be well applied to another study. For instance, it has been shown that findings of different AD study series (as ADNI, OASIS, AIBL, UKBiobank, PharmaCog etc.) well correlate to each other, and methodologies developed for one study (e.g. ADNI) can be translated to other studies (as OASIS, AIBL, PharmCog), and also to smaller local studies (as PMD dementia study) [37–39]. This translability corroborates and supports our approach for correlating the findings between the two aforesaid analysis set-ups (i) and (ii). Furthermore, our association of DTI parameter change (diffusivity) with the AD-affected regions of $A\beta_{42}$ deposition, is also substantiated by other researchers. For instance, it is known that in AD subjects, the change of MRI-DTI parameters (as diffusivity or anisotropy) satisfactorily correlates with PET-evaluated Aβ42 deposition in the brain [40,41].

To sum up, we may highlight that our analysis indicates a novel potential of hepatomodulative $A\beta_{42}$ excreting drugs towards a patient-specific personalized therapeutic approach depending on the neuroanatomical location of the pathology, i.e. the form of AD in the subject. It is well-known that AD actually shows a gamut of neurodegenerative behaviour, constituting the Alzheimer's spectrum, and the therapeutic response critically depends of the neuroanatomical form of AD [42]. Since conventional therapies aimed at cerebral $A\beta_{42}$ formation do not always have the desired effect in AD, it may be necessary to investigate alternative pathways. The recent multisystemic perspective of dementia delineates that AD is a hepatic metabolic encephalopathy [43], and this can furnish a unique prospect of intervening in AD from a metabolic framework.

5. Conclusion

We have delineated an innovative therapeutic perspective to Alzheimer's disease from one of its basic initial pathophysiological process, namely as a hepatic metabolic dysfunction affecting the brain, reminiscent of the generalized systems approach of metabolicencepahalopathies. Our neuroanatomical tractographic analysis, as far as we know, is the first pilot study in this direction. From a personalized medicine perspective, we show that patient-specific hepatomodulative drugs may a novel substantive therapeutic approach to Alzheimer's disease, according to the neuroanatomical form of AD, and that these pharmacological agents have the potentiality to target and activate the corresponding different affected tract networks which are dysfunctional in AD.

Supplementary Information

Documentation with Supplementary Materials, Supplementary Tables and Supplementary Figures.

CRediT authorship contribution statement

Anindita Bhattacharjee: Conceptualization, Data curation, Formal analysis, Investigation, Methodology, Software, Validation, Visualization, Writing – original draft, Writing – review & editing. **Prasun K. Roy:** Conceptualization, Formal analysis, Investigation, Methodology, Validation, Project administration, Visualization, Supervision, Writing – original draft, Writing – review & editing.

Declaration of competing interest

The authors declare that they have no known competing financial interests or personal relationships that could have appeared to influence the work reported in this paper.

Acknowledgements

PKR acknowledges the help of La Dassault Systemes Fondation, France, and The Royal Society, U. K., for support of the research. The authors are thankful for assistance from C3i Hub Foundation (sponsored by Dept. of Science & Technology, Govt. of India).

AB is obliged for research fellowships from Ministry of Education, India, through IIT (BHU). We appreciate the facilitation of SNU: Shiv Nadar University and IIT (BHU) for pursuing this work. We are grateful to the Respond scheme, Human Space Flight program, ISRO: Indian Space Research Organization, for assistance. The research sponsorship by NTTM Mission, Govt. of India, is thankfully recorded. Imaging acquisition were enabled by Alzheimer Disease Neuroimaging Initiative.

Supplementary materials

Supplementary material associated with this article can be found, in the online version, at doi:10.1016/j.dscb.2023.100112.

References

[1] Y. Cheng, C.-Y. He, D.-Y. Tian, S.-H. Chen, J.-R. Ren, H.-L. Sun, M.-Y. Xu, C.-R. Tan, D.-Y. Fan, J.-M. Jian, Physiological β-amyloid clearance by the liver and its therapeutic potential for Alzheimer's disease, Acta Neuropathol. 145 (2023) 717–731.
[2] J. Ghiso, M. Shayo, M. Calero, D. Ng, Y. Tomidokoro, S. Gandy, A. Rostagno, B. Frangione, Systemic catabolism of Alzheimer's Aβ40 and Aβ42, J. Biol. Chem. 279 (2004) 45897–45908.
[3] K. Nho, A. Kueider-Paisley, S. Ahmad, S. MahmoudianDehkordi, M. Arnold, S. L. Risacher, G. Louie, C. Blach, R. Baillie, X. Han, Association of altered liver enzymes with Alzheimer disease diagnosis, cognition, neuroimaging measures, and cerebrospinal fluid biomarkers, JAMA Netw. Open 2 (2019) e197978.
[4] R. Wiest, T. Weiss, L. Danielyan, C. Buechler, Serum amyloid beta-42 is not eliminated by the cirrhotic liver: a pilot study, J. Clin. Med. 10 (12) (2021) 2669, 1-8.
[5] N. Sehgal, A. Gupta, R.K. Valli, S.D. Joshi, J.T. Mills, E. Hamel, P. Khanna, S. C. Jain, S.S. Thakur, V. Ravindranath, Withania somnifera reverses Alzheimer's disease pathology by enhancing low-density lipoprotein receptor-related protein in liver, Proc. Natl Acad. Sci. 109 (2012) 3510–3515.
[6] A. Bhattacharjee, P.K. Roy, Conjoint hepatobiliary-enterohepatic cycles for amyloid excretion and enhancing its drug-induced clearance: a systems biology approach to Alzheimer's disease, J. Biomol. Struct. Dyn. (2022) 1–18.
[7] V. Pareek, S. Paul, V.S. Rallabandi, P.K. Roy, Patterning of corpus callosum integrity in glioma observed by MRI: effect of 2D bi-axial lamellar brain architecture, J. Neurooncol. 144 (2019) 165–177.
[8] A. Bhattacharjee, P. Purohit, P.K. Roy, Neuroprotective drug discovery from phytochemicals and metabolites for CNS viral infection: a systems biology approach with clinical and imaging validation, Front. Neurosci. 16 (2022).
[9] A. Raj, A. Kuceyeski, M. Weiner, A network diffusion model of disease progression in dementia, Neuron 73 (2012) 1204–1215.
[10] J. Zhou, E.D. Gennatas, J.H. Kramer, B.L. Miller, W.W. Seeley, Predicting regional neurodegeneration from the healthy brain functional connectome, Neuron 73 (2012) 1216–1227.
[11] S. Nath, L. Agholme, F.R. Kurudenkandy, B. Granseth, J. Marcusson, M. Hallbeck, Spreading of neurodegenerative pathology via neuron-to-neuron transmission of β-amyloid, J. Neurosci. 32 (2012) 8767–8777.

[12] T. Iizuka, K. Morimoto, Y. Sasaki, M. Kameyama, A. Kurashima, K. Hayasaka, H. Ogata, H. Goto, Preventive effect of rifampicin on Alzheimer disease needs at least 450mg daily for 1 year: an FDG-PET follow-up study, Dement. Geriatr. Cogn. Dis. Extra 7 (2017) 204–214.
[13] A.M. Koenig, D. Mechanic-Hamilton, S.X. Xie, M.F. Combs, A.R. Cappola, L. Xie, J. A. Detre, D.A. Wolk, S.E. Arnold, Effects of the insulin sensitizer metformin in Alzheimer's disease: pilot data from a randomized placebo-controlled crossover study, Alzheimer Dis. Assoc. Disord. 31 (2017) 107.
[14] J.-Y. Lee, H. Lee, H.B. Yoo, J.-S. Choi, H.-Y. Jung, E.J. Yoon, H. Kim, Y.-H. Jung, H.-Y. Lee, Y.K. Kim, Efficacy of cilostazol administration in alzheimer's disease patients with white matter lesions: a positron-emission tomography study, Neurotherapeutics 16 (2019) 394–403.
[15] R.C. Petersen, P.S. Aisen, L.A. Beckett, M.C. Donohue, A.C. Gamst, D.J. Harvey, C. R. Jack, W.J. Jagust, L.M. Shaw, A.W. Toga, Alzheimer's disease neuroimaging initiative (ADNI): clinical characterization, Neurology 74 (2010) 201–209.
[16] P.S. Aisen, R.C. Petersen, M.C. Donohue, A. Gamst, R. Raman, R.G. Thomas, S. Walter, J.Q. Trojanowski, L.M. Shaw, L.A. Beckett, Clinical core of the Alzheimer's disease neuroimaging Initiative: progress and plans, Alzheimer's Dement. 6 (2010) 239–246.
[17] B.L. Edlow, E. Takahashi, O. Wu, T. Benner, G. Dai, L. Bu, P.E. Grant, D.M. Greer, S. M. Greenberg, H.C. Kinney, Neuroanatomic connectivity of the human ascending arousal system critical to consciousness and its disorders, J. Neuropathol. Exp. Neurol. 71 (2012) 531–546.
[18] F.C. Yeh, L. Liu, T.K. Hitchens, Y.L. Wu, Mapping immune cell infiltration using restricted diffusion MRI, Magn. Reson. Med. 77 (2017) 603–612.
[19] J. Schmahmann, D. Pandya, Fiber pathways of the brain, Oxford University Press, New York, 2009.
[20] A. Kobro-Flatmoen, M.J. Lagartos-Donate, Y. Aman, P. Edison, M.P. Witter, E. F. Fang, Re-emphasizing early Alzheimer's disease pathology starting in select entorhinal neurons, with a special focus on mitophagy, Ageing Res. Rev. 67 (2021) 101307.
[21] E. Levitis, J.W. Vogel, T. Funck, V. Hachinski, S. Gauthier, J. Vöglein, J. Levin, B. A. Gordon, T. Benzinger, Y. Iturria-Medina, Differentiating amyloid beta spread in autosomal dominant and sporadic Alzheimer's disease, Brain Commun. 4 (2022) fcac085.
[22] H. Braak, E. Braak, Neuropathological stageing of Alzheimer-related changes, Acta Neuropathol. 82 (1991) 239–259.
[23] J.P. Aggleton, A. Pralus, A.J. Nelson, M. Hornberger, Thalamic pathology and memory loss in early Alzheimer's disease: moving the focus from the medial temporal lobe to Papez circuit, Brain 139 (2016) 1877–1890.
[24] R.L. Buckner, J.R. Andrews-Hanna, D.L. Schacter, The brain's default network: anatomy, function, and relevance to disease, Ann. N. Y. Acad. Sci. 1124 (2008) 1–38.
[25] S. Minoshima, B. Giordani, S. Berent, K.A. Frey, N.L. Foster, D.E. Kuhl, Metabolic reduction in the posterior cingulate cortex in very early Alzheimer's disease, Ann. Neurol. 42 (1997) 85–94.
[26] Gorijala, P., Nho, K., Risacher, S.L., Kaddurah-Daouk, R., Saykin, A.J., Yan, J., 2020. Functional biological paths altered in Alzheimer's disease: from genes to bile acids. Biorxiv. 2020.01. 31.929554 10.1101/2020.01.31.929554.
[27] M.P. Coleman, M.R. Freeman, Wallerian degeneration, wlds, and nmnat, Annu. Rev. Neurosci. 33 (2010) 245–267.
[28] N. Vats, R. Dubey, S. Girija, S. Venugopal, Glibenclamide Glibenclamide, ATP and metformin increases the expression of human bile salt export pump, F1000Res. 9 (2020) 1–17.
[29] K. Lunnon, R. Smith, E. Hannon, P.L. De Jager, G. Srivastava, M. Volta, C. Troakes, S. Al-Sarraj, J. Burrage, R. Macdonald, Methylomic profiling implicates cortical deregulation of ANK1 in Alzheimer's disease, Nat. Neurosci. 17 (2014) 1164–1170.
[30] J.E. Park, G. Ryoo, W. Lee, Alternative splicing: expanding diversity in major ABC and SLC drug transporters, AAPS J. 19 (2017) 1643–1655.
[31] G. Yeo, D. Holste, G. Kreiman, C.B. Burge, Variation in alternative splicing across human tissues, Genome Biol. 5 (10) (2004) R74.
[32] E.S. White, F.E. Baralle, A.F. Muro, New insights into form and function of fibronectin splice variants, J. Pathol. 216 (2008) 1–14.
[33] A. Brenn, M. Grube, M. Peters, A. Fischer, G. Jedlitschky, H.K. Kroemer, R. W. Warzok, S. Vogelgesang, Beta-amyloid downregulates MDR1-P-glycoprotein (Abcb1) expression at the blood-brain barrier in mice, Int. J. Alzheimer's Dis. 2011 (2011).
[34] N.F. Fitz, A.A. Cronican, M. Saleem, A.H. Fauq, R. Chapman, I. Lefterov, R. Koldamova, Abca1 deficiency affects Alzheimer's disease-like phenotype in human ApoE4 but not in ApoE3-targeted replacement mice, J. Neurosci. 32 (2012) 13125–13136.
[35] L.D. Estrada, P. Ahumada, D. Cabrera, J.P. Arab, Liver dysfunction as a novel player in Alzheimer's progression: looking outside the brain, Front. Aging Neurosci. 11 (2019) 174.
[36] B. Zhang, L. Lin, S. Wu, Z.H. Al-Masqari, Multiple subtypes of Alzheimer's disease base on brain atrophy pattern, Brain Sci 11 (2021) 278.
[37] L. Bloch, C.M. Friedrich, A.s.D.N. Initiative, Machine learning workflow to explain black-box models for early Alzheimer's disease classification evaluated for multiple datasets, SN Comput. Sci. 3 (2022) 509.
[38] E.E. Bron, S. Klein, J.M. Papma, L.C. Jiskoot, V. Venkatraghavan, J. Linders, P. Aalten, P.P. De Deyn, G.J. Biessels, J.A. Claassen, Cross-cohort generalizability of deep and conventional machine learning for MRI-based diagnosis and prediction of Alzheimer's disease, NeuroImage 31 (2021) 102712.
[39] A. Tam, C. Laurent, S. Gauthier, C. Dansereau, Prediction of cognitive decline for enrichment of Alzheimer's disease clinical trials, J. Prev. Alzheimers Dis. (2022) 1–10.
[40] A. Moscoso, J. Silva-Rodríguez, J.M. Aldrey, J. Cortés, J.M. Pías-Peleteiro, A. Ruibal, P. Aguiar, A.s.D.N. Initiative, 18 F-florbetapir PET as a marker of myelin integrity across the Alzheimer's disease spectrum, Eur. J. Nucl. Med. Mol. Imaging (2022) 1–12.
[41] A.M. Racine, N. Adluru, A.L. Alexander, B.T. Christian, O.C. Okonkwo, J. Oh, C. A. Cleary, A. Birdsill, A.T. Hillmer, D. Murali, Associations between white matter microstructure and amyloid burden in preclinical Alzheimer's disease: a multimodal imaging investigation, NeuroImage 4 (2014) 604–614.
[42] H.H. Fudenberg, V.K. Singh, Alzheimer's "syndrome": prognosis of subsets with different etiology and preliminary effects of immunotherapy, Drug Dev. Res. 15 (1988) 165–174.
[43] M.F. Bassendine, S.D. Taylor-Robinson, M. Fertleman, M. Khan, D. Neely, Is Alzheimer's disease a liver disease of the brain? J. Alzheimers Dis. (2020) 1–14.